

## MICROWAVE MIXER ON RECTANGULAR WAVEGUIDES PARTIALLY FILLED BY DIELECTRIC

Vitaly Pochernyaev<sup>1</sup>, Nataliia Syvkova<sup>1</sup>, Mariia Mahomedova<sup>2</sup>

<sup>1</sup>National Academy of Security Service of Ukraine, Kyiv, Ukraine, <sup>2</sup>Kyiv Professional College of Communications, Kyiv, Ukraine

**Abstract.** The article investigates and calculates the characteristics of microwave mixers on rectangular waveguides partially filled by dielectric. Presents diagrams of promising combined microwave radio engineering systems - two options for constructing mobile digital troposcatter-radiorelay stations, the antenna-feeder paths of which are implemented on rectangular waveguides partially filled by dielectric. At research of microwave mixers, suppression and the use of the mirror frequency are taken into account. The analysis of researches of microwave mixers is carried out. The design of a balanced-type microwave mixer based on rectangular waveguides partially filled by dielectric is developed. The mixer is used to convert the microwave signal into an intermediate frequency signal. The signal conversion of the mixers takes place on the non-linear active resistance of the semiconductor diode. In article, an open nonlinear structure is used as such a diode. The following main parameters of microwave mixers are investigated: conversion losses, noise factor, operating frequency band, signal suppression at the mirror frequency. The conversion losses are determined for various mirror channel suppression conditions. Phase methods of mirror frequency suppression are considered, which are most suitable for the waveguide implementation of microwave mixers. A scheme of a microwave mixer of a balance type with a phase method for suppressing the mirror frequency is presented. The article notes that for significant suppression of the mirror frequency of more than 30 dB, a double frequency conversion mixer is used. A diagram of a slotted bridge based on rectangular waveguides partially filled by dielectric is presented. The dependences of the input impedance of the mixer, the impedance of the mixer at the intermediate frequency, the impedance of the mixer at the mirror frequency by the power of the local heterodyne are plotted.

**Keywords:** microwave mixer, mobile digital troposcatter-radiorelay station, rectangular waveguide, slot bridge, conversion loss, mirror frequency

## MIKSER MIKROFALOWY NA PROSTOKĄTNYCH FALOWODACH CZĘŚCIOWO WYPEŁNIONYCH DIELEKTRYKIEM

**Streszczenie.** W artykule zbadano i obliczono charakterystyki mieszaczy mikrofalowych na falowodach prostokątnych częściowo wypełnionych dielektrykiem. Przedstawiono schematy obiecujących połączonych mikrofalowych systemów inżynierii radiowej – dwóch opcji budowy mobilnych cyfrowych troposferycznych stacji radiowych, których tory antenowo-zasilające są realizowane na prostokątnych falowodach częściowo wypełnionych dielektrykiem. W badaniach mieszaczy mikrofalowych uwzględniono tłumienie i wykorzystanie częstotliwości lustrzanej. Przeprowadzono analizę badań mieszaczy mikrofalowych. Opracowano projekt mieszacza mikrofalowego typu zrównoważonego opartego na prostokątnych falowodach częściowo wypełnionych dielektrykiem. Mieszacz służy do konwersji sygnału mikrofalowego na sygnał o częstotliwości pośredniej. Konwersja sygnału mieszacza odbywa się na nieliniowej rezystancji czynnej diody półprzewodnikowej. W artykule jako taką diodę zastosowano otwartą strukturę nieliniową. Badane są następujące główne parametry mieszaczy mikrofalowych: straty konwersji, współczynnik szumów, pasmo częstotliwości roboczej, tłumienie sygnału na częstotliwości lustrzanej. Straty konwersji są określane dla różnych warunków tłumienia kanału lustrzanego. Rozważono fazowe metody tłumienia częstotliwości lustrzanej, które są najbardziej odpowiednie do falowodowej implementacji mieszaczy mikrofalowych. Przedstawiono schemat mieszacza mikrofalowego typu balansowego z fazową metodą tłumienia częstotliwości lustrzanej. W artykule zauważono, że w celu znacznego tłumienia częstotliwości lustrzanej o ponad 30 dB stosuje się mieszacz z podwójną konwersją częstotliwości. Przedstawiono schemat mostka szczelinowego opartego na prostokątnych falowodach częściowo wypełnionych dielektrykiem. Wykreślono zależności impedancji wejściowej mieszacza, impedancji mieszacza dla częstotliwości pośredniej, impedancji mieszacza dla częstotliwości lustrzanej od mocy lokalnej heterodyny.

**Słowa kluczowe:** mieszacz mikrofalowy, mobilna cyfrowa troposferyczna stacja radiowa, falowód prostokątny, mostek szczelinowy, straty konwersji, częstotliwość lustrzana

### Introduction

In areas of natural disasters and man-made disasters, in the event of emergency and emergency situations, as well as in the conditions of hostilities or special ground operations, the most likely option for organizing a terrestrial communication line in the microwave range may be to build a combination of troposcatter and radiorelay communication stations. At present, despite the widespread use of satellite communication systems, troposcatter stations are used both in special-purpose networks and in departmental and corporate networks. Higher survivability in a difficult jamming environment is an advantage of troposcatter communications over other microwave radio systems, including satellite ones [1–3, 6, 7, 17–20].

Schemes of mobile digital troposcatter-radiorelay stations (MDTRRS), which are combined microwave radio systems, are shown in Fig. 1 and Fig. 2 [12, 13]. Such a combined microwave radio system provides an over-the-horizon communication mode in the presence of a troposcatter component and a line-of-sight mode in the presence of a radiorelay component, which makes it possible to build a transport network with different distances between control and relay points.

On Fig. 1 shows the microwave transceiver path of a MDTRRS (option 1), where: *I* and *II* – antennas of troposcatter component; *A* and *B* – antennas of radiorelay component; *V* and *H* – vertical and horizontal polarization; *PS 1TC* and *PS 2TC* – polarization selectors of troposcatter component; *D1* and *D2* – duplexers; *DP* – distributor of power; *PD1* and *PD2* – power dividers; *FBFET 1*, *FBFET 2*, *FBFET 3*

and *FBFET 4*, – frequency bandpass filters with electronically tunable; *MR 1TC*, *MR 2TC*, *MR 3TC* and *MR 4TC* – microwave receivers of troposcatter component; *MM 1TC*, *MM 2TC*, *MM 3TC* and *MM 4TC* – microwave mixers of troposcatter component; *PS 1RC* and *PS 2RC* – polarization selectors of radiorelay component; *EH* – exciter-heterodyne; *OBFFT 1RC* and *OBFFT 2RC* – output bandpass filters with frequency tunable of radiorelay component; *MR 1RC*, *MR 2RC* – microwave receivers of radiorelay component; *MM 1RC* and *MM 2RC* – microwave mixers of radiorelay component; *MT1* and *MT2* – microwave transmitters; *CP* – control panel; *DSTC* – device of space-time coding; *PIFA1*, *PIFA2*, *PIFA3* and *PIFA4* – previous intermediate frequency amplifier; *M* – modem; *M-D RC* – multiplexer-demultiplexer of radiorelay component, *S1*, *S2* – switch, *SCP1*, *SCP2* – switch control panel.

Figure 2 shows the microwave transceiver path of a MDTRRS (option 2), where: *I* and *II* – antennas of troposcatter component; *A* and *B* – antennas of radiorelay component; *V* and *H* – vertical and horizontal polarization; *PS 1TC* and *PS 2TC* – polarization selectors of troposcatter component; *D1* and *D2* – duplexers; *DP* – distributor of power; *BFFT 1*, *BFFT 2*, *BFFT 3* and *BFFT 4* – bandpass filters with frequency tunable; *MR 1TC*, *MR 2TC*, *MR 3TC* and *MR 4TC* – microwave receivers of troposcatter component; *MM 1TC*, *MM 2TC*, *MM 3TC* and *MM 4TC* – microwave mixers of troposcatter component; *PS 1RC* and *PS 2RC* – polarization selectors of radiorelay component; *OBFFT 1RC* and *OBFFT 2RC* – output bandpass filters with frequency tunable of radiorelay component; *RT 1RC* and *RT 2RC* – receiver-transmitter of radiorelay component; *EA*

*ITC* and *EA 2TC* – equivalents antennas of troposcatter component; *MT 1TC* and *MT 2TC* – microwave transmitters of troposcatter component; *EH* – exciter-heterodyne; *PIFA1*, *PIFA2*, *PIFA3* and *PIFA4* – previous intermediate frequency amplifier; *M-D RC* – multiplexer-demultiplexer of radiorelay component; *M* – modem; *AC* – automatic control; *PAS* – power adaptation system; *FAS* – frequency adaptation system; *DSTC* – device of space-time coding.

To reduce the weight and size parameters and increase the electrical strength, the microwave paths of such stations can be implemented on rectangular waveguide partially filled by dielectric (RWPFD). However, a complete range of active devices based on RWPFD has not been developed, including microwave mixers. The schemes on Fig.1, 2 contain a six microwave mixers.

The aim of the article is to research the characteristics and parameters of microwave mixers on RWPFD.

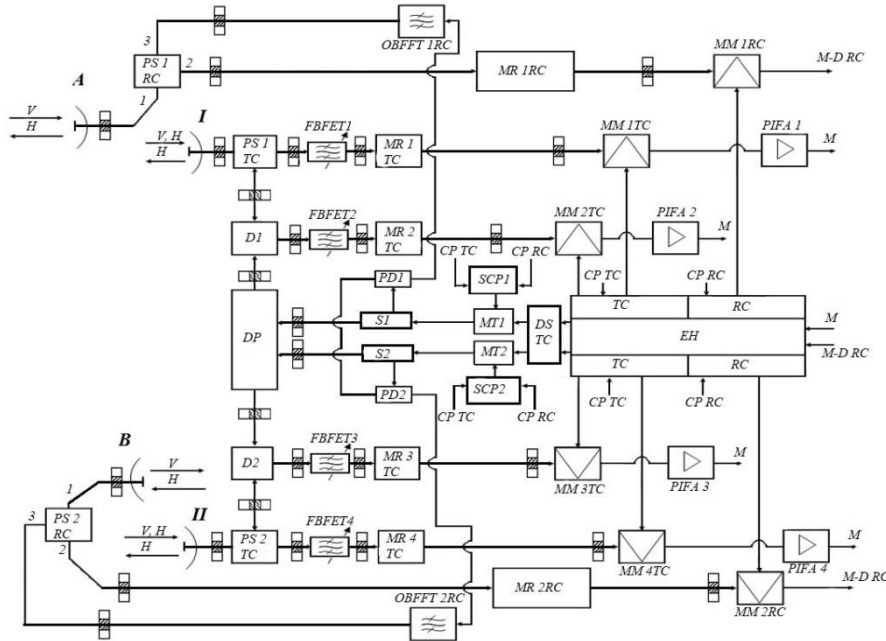


Fig. 1. Transmitting and receiving microwave paths MDTRRS (option 1)

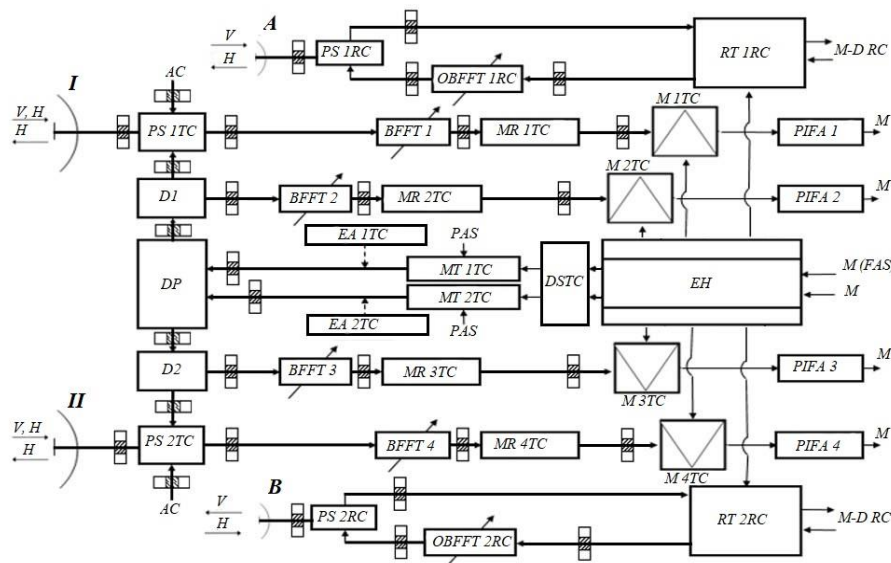


Fig. 2. Transmitting and receiving microwave paths MDTRRS (option 2)

### 1. Analysis of microwave mixer research

The performed analysis of mixers shows that studies will be introduced in low noise directions for software defined radios [15, 16]. The most promising "technique" in the suppression of the mirror frequency is the phase method [5, 9, 11]. The technique for measuring the characteristics and parameters of mixer models, microwave and extremely high frequencies ranges is based on the use of a digital signal generator and a spectrum analyzer described in [4]. The results of experimental studies of promising designs of balanced microwave mixers are given in [8].

### 2. Main part

A microwave mixer is needed to convert the microwave signal into an intermediate frequency (IF) signal. The conversion of the mixer signal occurs on the active non-linear resistance of the semiconductor diode. In this article, an open non-linear structure (ONS) is used as a semiconductor diode, placed in a dielectric plate RWPFD. The following main characteristics and parameters of the microwave mixer were studied: conversion loss, noise factor, operating frequency band, suppression of the mirror channel. This study does not include the study of the combinational components suppression, but only considers the suppression and the use of the mirror frequency (mirror channel).

On Fig. 3 shows the design of the microwave mixer at RWPFDD: a) - general view; b) - face view; c) top view.

The design of the balanced mixer at RWPFDD is shown in Fig. 3.

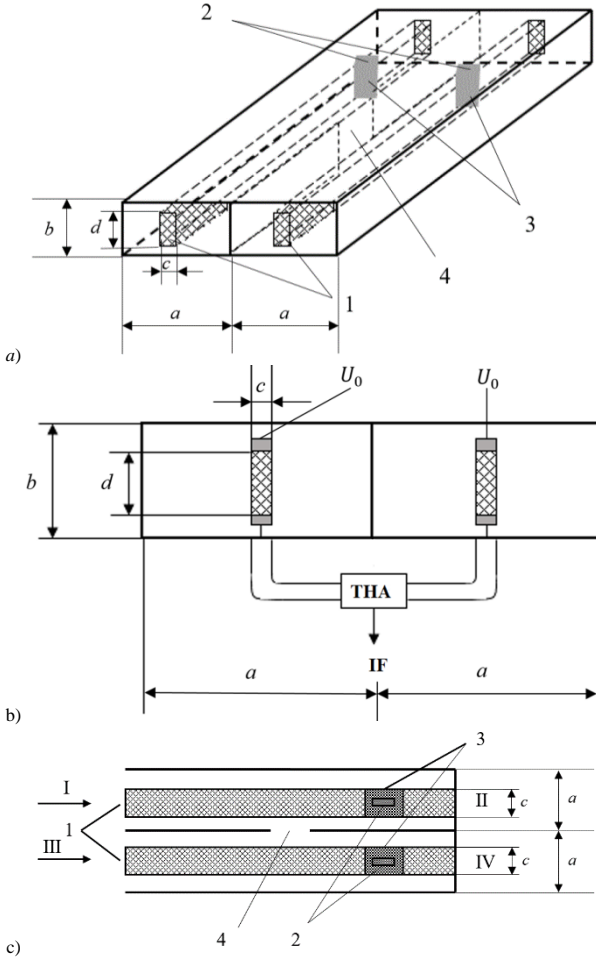


Fig. 3. Slotted bridge on RWPFDD: 1- dielectric plates; 2 - non-radiating slots; 3 - open nonlinear structures; 4 - connection hole

Inputs I and III are supplied with a useful signal and a local heterodyne signal, respectively. Outputs II and IV are shorted, the control voltage  $U_0$  is supplied through the non-radiating slots 2. The connection hole 4 provides the local heterodyne signal with an additional phase shift  $\pi/2$ . In the second channel, the additional phase shift  $\pi/2$  through the connection hole 4 acquires a useful signal. Therefore, the instantaneous phases of the IF currents on the first and second ONS are equal:

$$\varphi_1 = \left( \varphi_h - \frac{\pi}{2} \right) - \varphi_s, \quad \varphi_2 = \varphi_h - \left( \varphi_s - \frac{\pi}{2} \right)$$

From this it can be seen that the phases  $\varphi_1$  and  $\varphi_2$  differ by  $\pi$ , therefore, when the ONS is turned on in the opposite direction, we get the addition of currents at the input of the IF amplifier. Note that the noise oscillations turn out to be in-phase and, when the ONS are connected back to back, are mutually compensated. Balanced circuit makes it easier to tune the mixer and increases the decoupling of the signal and heterodyne frequencies.

On Fig. 4 shows a diagram of a transformer hybrid adder (THA) used as an adder and a matching device.

The circuit in Fig. 4 makes it possible to implement a wide range of matched resistances  $r$  with relatively small and quite acceptable values of  $n$  and  $k$  from the point of view of obtaining wide bandwidths. This scheme, when using two identical transformers with those indicated in Fig. 4 transformation ratios works in a symmetrical version at  $n = 1 \pm \sqrt{2}$ .

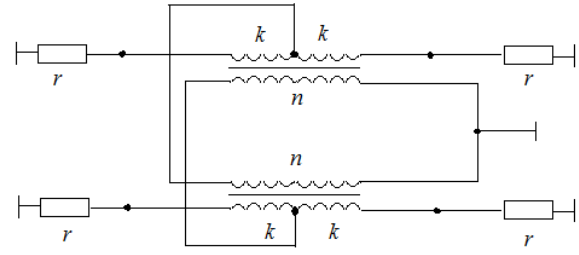


Fig. 4. Scheme of THA

The frequency range of the developed slotted bridge on RWPFDD, as well as the microwave mixer, is determined by:

$$\frac{2\Delta\lambda}{\lambda_0} \approx \left( \frac{2\Delta\theta}{\theta_0} \right) \left[ \left( \varepsilon_{eff1} - \left( \frac{\lambda_0}{2a} \right)^2 \right) \left( \varepsilon_{eff2} - \left( \frac{\lambda_0}{4a} \right)^2 \right) \right]^{1/2} \quad (1)$$

$$\varepsilon_{eff1} = 1 + (\varepsilon_r - 1) \frac{cd}{ab} \left[ 1 + \frac{\sin(\pi c/a)}{\pi c/a} \right]$$

$$\varepsilon_{eff2} = 1 + (\varepsilon_r - 1) \frac{cd}{ab} \left[ 1 - \frac{\sin(2\pi c/a)}{2\pi c/a} \right]$$

where  $\lambda_0$  - frequency band center wavelength;  $2\Delta\theta/\theta_0$  - value specifying the level of crosstalk to be set;  $\varepsilon_{eff1}$ ,  $\varepsilon_{eff2}$  - effective permittivity of quasi- $H_{10}$  and quasi- $H_{20}$  waves, respectively;  $a$ ,  $b$  - dimensions of a rectangular waveguide;  $c$ ,  $d$  - dimensions of the dielectric plate;  $\varepsilon_r$  - relative permittivity of a dielectric plate.

The values  $2\Delta\theta/\theta_0$  can be found using the following expressions:

$$\Delta\theta = \arcsin 10^{-0.05(\alpha-\Delta\alpha)} - \arcsin 10^{-0.05(\alpha+\Delta\alpha)}$$

$$\theta_0 = (2n-1)\pi/2, \quad n=1,2,3,\dots$$

A standard waveguide slot bridge (WSB) on empty rectangular waveguides has a bandwidth of 9.2%. The throughput capacity of the developed WSB on RWPFDD with dimensions  $c/a = 0.12$  and  $d/b = 0.8$  according to formula (1) is as follows:

- for  $\varepsilon_r = 2.4$  we have  $2\Delta\lambda/\lambda_0 = 10.8\%$
- for  $\varepsilon_r = 4$  we have  $2\Delta\lambda/\lambda_0 = 12.4\%$
- for  $\varepsilon_r = 9.6$  we have  $2\Delta\lambda/\lambda_0 = 17.1\%$

Let's move on to the analysis of other main parameters of the mixer. The mixer conversion loss  $L_s$  is defined as the ratio of the input power of the microwave signal  $P_{in,s}$  to the output power of the signal at the intermediate frequency  $P_{IF}$ . Losses are usually expressed in decibels:

$$L_s = 10 \lg(P_{in,s} / P_{IF})$$

The mixer conversion losses consist of the ONS conversion losses  $L_d$ , the losses of the ONS inconsistency at the input and output, as well as losses in the passive elements of the mixer, for example, a slotted bridge.

The conversion loss  $L_d$  is related to the properties of the semiconductor material in such a way:

$$L_d \sim \sqrt{\varepsilon_d}$$

where  $\varepsilon_d$  - relative dielectric permittivity ONS.

Noise factor:

$$K_N = 10 \lg \frac{P_{in,s} / P_{in,N}}{P_{out,s} / P_{out,N}}$$

where  $P_{in,s}$  and  $P_{out,s}$  - nominal input and output signal power;  $P_{in,N}$  and  $P_{out,N}$  - nominal input and output noise power.

The noise factor of the mixer is a generalized parameter that takes into account the noise factor of the ONS  $K_{N,d}$  and conversion losses, as well as the noise factor of the intermediate frequency amplifier (IFA)  $K_{N,IFA}$ . The noise factor of a mixer with IFA is described by the equation:  $K_N = L_S(K_{N,d} + K_{N,IFA} - 1)$ .

Usually  $K_{N,IFA} = 1.4$  (or 1.5 dB).

Suppression of the mirror channel is determined by the ratio of the signal power of the IF to the signal power on the mirror channel  $P_m$  and is expressed in decibels:

$$K_{p,m} = 10 \lg(P_{IF} / P_m)$$

The conversion losses can be determined using the theory of linear electrical circuits. In the simplest case, it is assumed that the following changes in nonlinear conductivity occur in the ONS under the influence of the local heterodyne voltage:

$$g = g_0 + 2 \sum_{n=1}^{\infty} g_n \cos n\omega t \quad (2)$$

where  $\omega$  – oscillation frequency of the local heterodyne;  $g_0$  – the constant component of the conductivity of the ONS;  $g_n$  – fourier component of conductivity at frequencies  $n\omega$ .

To determine the transformation losses, introduce the notation:

$$\gamma_n = g_n / g_0$$

Determine the conversion loss for different conditions for suppressing the mirror channel:

– the mirror channel is matched to the load:

$$L_m = 2(1 + \sqrt{1 - \eta_c}) / (1 - \sqrt{1 - \eta_c}), \eta_c = 2\gamma_1^2 / (1 + \gamma_2)$$

– the mirror channel on a short-circuited load:

$$L_m = (1 + \sqrt{1 - \eta_k}) / (1 - \sqrt{1 - \eta_k}), \eta_k = \gamma_1^2$$

– the mirror channel on open load:

$$L_m = (1 + \sqrt{1 - \eta_p}) / (1 - \sqrt{1 - \eta_p}), \eta_p = \gamma_1^2(1 - \gamma_2) / (1 - \gamma_1^2)(1 + \gamma_2)$$

Determine the input conductivity depending on the load of the mirror channel:

– the mirror channel is matched to the load:

$$g_m = g_0 \sqrt{(1 - \gamma_2)(1 + \gamma_2 - 2\gamma_1^2)}$$

– the mirror channel on a short-circuited load:

$$g_m = g_0 \sqrt{(1 - \gamma_1^2)}$$

– the mirror channel on open load:

$$g_m = g_0 \sqrt{(1 - \gamma_2^2) \sqrt{(1 - \gamma_2)(1 + \gamma_2 - 2\gamma_1^2)} / (1 - \gamma_1^2)}$$

Determine the IF conductivity:

– the mirror channel matched to the load:

$$g_{our} = g_0 \sqrt{(1 + \gamma_2 - 2\gamma_1^2) / (1 + \gamma_2)}$$

– the mirror channel on a short-circuited load:

$$g_{our} = g_0 \sqrt{(1 - \gamma_1^2)}$$

– the mirror channel on open load:

$$g_{our} = g_0 \sqrt{(1 - \gamma_2^2)^2 (1 + \gamma_2 - 2\gamma_1^2) / (1 - \gamma_1^2)}$$

If the indicated values are calculated with a short-circuited load through the mirror channel, i.e.  $Y_m = \infty$ , then the impedance of the mixer IF is lower resistance than with a matched load and an open channel of the mirror frequency. This does not require agreement with the previous IFA (PIFA). Therefore, the noise factor of the mixer with PIFA is lower, although theoretically the mixer conversion loss with an open channel of the mirror frequency is less than with a short-circuited one. In this case, the ONS is a symmetrical four-terminal network and its initial conductivity is equal to the conductivity at the IF.

Taking into account only the frequencies (signal, intermediate, mirror) and conductivity according to formula (2), we obtain the complex conductivity matrix of the ONS:

$$\begin{bmatrix} g_0 + ja_0\omega_s & g_1 + ja_1\omega_s & g_2 + ja_2\omega_s \\ g_{-1} + ja_{-1}\omega_{IF} & g_0 + ja_0\omega_{IF} & g_1 + ja_1\omega_{IF} \\ g_{-2} + ja_{-2}\omega_m & g_{-1} + ja_{-1}\omega_m & g_0 + ja_0\omega_m \end{bmatrix} \quad (3)$$

where  $\omega_s = \omega_{IF} + \omega_h$ ;  $\omega_m = \omega_h + \omega_{IF}$ .

The conductivities included in matrix (3) are calculated according to the method of [10]. Note that two waves quasi- $H_{10}$  and quasi- $H_{20}$  propagate in the coupling region of the slot bridge. In the calculation of reactive conductivities, the main contribution to the formation of the local field is made by the quasi- $H_{30}$  wave.

The transverse electrical eigenfunctions of these waves, through which the conductivities of matrix (3) are determined written as follows:

$$\bar{\mathcal{E}}_{h_{30}} = \left( \sqrt{128 / ab(64 + q^2 + p^2 + q^2 p^2)} / \chi_{h_{30}} \right) * \mathcal{F}$$

$$\mathcal{F} = \left\{ \left[ \left( \frac{\pi}{a} \right) \sin \frac{\pi x}{a} - \left( \frac{p\pi}{2a} \right) \sin \frac{\pi x}{a} \cos \frac{2\pi y}{b} - \left( \frac{3q\pi}{ba} \right) * \sin \frac{3\pi x}{a} \sin \frac{\pi x}{a} \cos \frac{2\pi y}{b} - \left( \frac{3q\pi}{ba} \right) \sin \frac{3\pi x}{a} + \left( \frac{3qp\pi}{16a} \right) \sin \frac{3\pi x}{a} \cos \frac{2\pi y}{b} \right] \bar{y}^0 + \left[ \left( \frac{p\pi}{b} \right) \cos \frac{\pi x}{a} * \sin \frac{2\pi y}{b} - \left( \frac{2qp\pi}{8b} \right) \cos \frac{3\pi x}{a} \sin \frac{2\pi y}{b} \right] \bar{x}^0 \right\}$$

$$\bar{\mathcal{E}}_{h_{20}} = \left( \sqrt{128 / ab(64 + q^2 + p^2 + q^2 p^2)} / \chi_{h_{20}} \right) *$$

$$\left\{ \left[ p\tau \cos 2\delta x \sin 2\tau y - \left( \frac{qp\tau}{8} \right) Q_1 \sin 2\tau y \right] \bar{x}_0 + (2\delta \sin 2\delta x - p\delta \sin 2\delta x \cos 2\tau y - \left( \frac{q\delta}{3} \right) \sin 4\delta x \cos 2\tau y) \bar{y}_0 \right] Q_1 = \frac{2}{3} \cos 4\delta x - 2$$

$$\bar{\mathcal{E}}_{h_{10}} = \sqrt{128 / ab(64 + q^2 + p^2 + q^2 p^2)} * \frac{1}{k_{h_{10}}} * \mathcal{J}$$

$$\mathcal{J} = \left\{ \left[ \frac{p\pi}{b} \cos \frac{3\pi x}{a} \sin \frac{2\pi y}{b} - \frac{qp\pi}{16b} \left( \cos \frac{5\pi x}{a} - 2\cos \frac{\pi x}{a} \right) * \sin \frac{2\pi y}{b} \right] \bar{x}^0 + \left[ \frac{3\pi}{a} \sin \frac{3\pi x}{a} - \frac{3p\pi}{2a} \sin \frac{3\pi x}{a} \cos \frac{2\pi y}{b} - \frac{q\pi}{8a} \left( \frac{5}{2} \sin \frac{5\pi x}{a} - \sin \frac{\pi x}{a} \right) + \frac{qp\pi}{16a} \left( \frac{5}{2} \sin \frac{5\pi x}{a} - \sin \frac{\pi x}{a} \right) \cos \frac{2\pi y}{b} \right] \bar{y}^0 \right\}$$

where  $\chi_{h_{10}}$ ,  $\chi_{h_{20}}$ ,  $\chi_{h_{30}}$  – transverse wavenumbers of waves quasi- $H_{10}$ , quasi- $H_{20}$ , quasi- $H_{30}$  [20].

Consider phase methods for suppressing mirror frequencies.

So, for example, four branches of the receiver of the tropo-scatter component of the MDTRRS contain four microwave mixers (Fig. 1, 2). In addition to the main conversion in microwave mixers, there is a parasitic conversion to the frequency of the mirror channel.

The appearance of the mirror channel occurs due to the transmission of the signal range from one radio frequency region to another. In the scheme of the balance-type mixer in Fig. 5, a microwave mixer is used, which is shown in Fig. 3. The circuit in Fig. 5 should be highly symmetrical. In this case, the suppression of the mirror channel is carried out by the phase method.

If the phase of the converted signal is shifted by less than 5 degrees, and when the signal amplitude difference is 1 dB from two non-linear elements, then the microwave mixer circuit can suppress the mirror frequency signal by 25 dB.

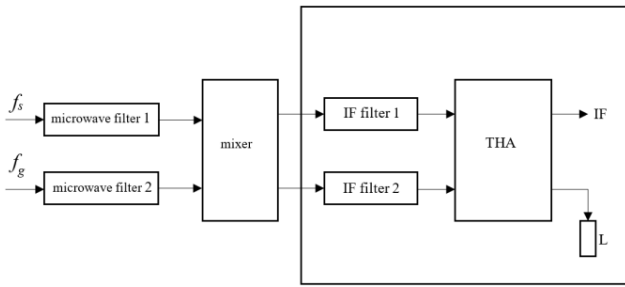


Fig. 5. Scheme of a microwave mixer of a balance type with a phase method of suppression

The scheme in Fig. 5 includes: IF filter 1, IF filter 2 – intermediate frequency filters; L – load; IF – intermediate frequency; THA – transformer hybrid adder. The mixer is built according to the design of Fig. 3.

The loss  $L_m$  conversion of mirror frequency is a function of factor  $K_m$  conversion the signal to mirror frequency:

$$K_m = (P_m / P_s) \cos [2\pi(2f_s - f_{sf})t + (2\varphi_s - \varphi_{sf})]$$

where  $P_m$  – power of mirror frequency;  $P_s$  – input signal power;  $f_s$  – input signal frequency;  $f_{sf}$  – frequency synthesizer frequency;  $\varphi_s$  – input signal phase;  $\varphi_{sf}$  – frequency synthesizer signal phase.

It should be taken into account that the conversion loss and therefore the efficiency of the mirror frequency signal suppression, depends on the characteristics of the non-linear elements.

On Fig. 6 shows a fragment of the IF included in the microwave mixer of the balanced type. The addition of devices for controlling and controlling the amplitude and phase (APCMD 1, APCMD 2) makes it possible to improve the suppression of the mirror channel.

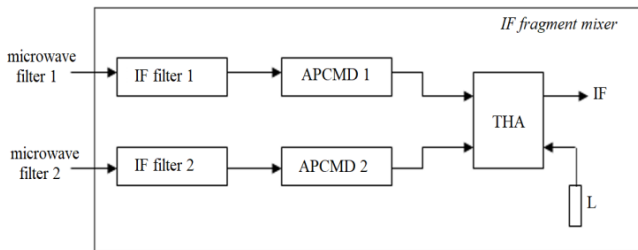


Fig. 6. Fragment of the IF included in the microwave mixer of the balance type with the phase method of suppression

These devices make it possible to provide a phase deviation of 1 degree from two non-linear elements and an amplitude of their difference of 0.1 dB. This allows an additional 15 dB of mirror frequency rejection to be added. Therefore, the total rejection of the mirror frequency signal using APCMD 1, APCMD 2 is approximately 40 dB.

The dependence of losses  $L_m$  and  $L_s$  in the frequency range is shown in Fig. 7.

Note that if significant mirror frequency rejection of more than 30 dB is required, a double frequency conversion mixer is used. Such a scheme is implemented by switching on two mixers in series: the first one transfers the signal to the high first IF, at which it is easy to suppress the mirror frequency with filters, and then the second mixer turns the high IF into a low IF, on which further signal processing takes place. Note that the frequency range in Fig. 7 corresponds to the frequency range of a mobile digital troposcatter station.

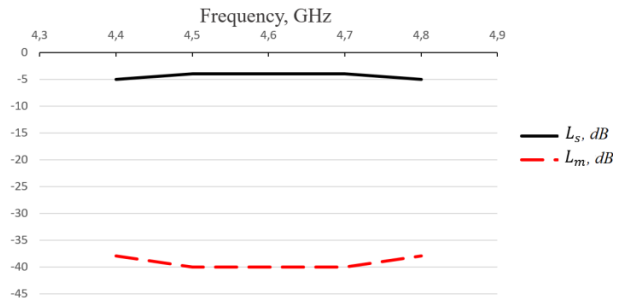


Fig. 7. Dependence of losses  $L_m$  and  $L_s$  in the frequency range

To obtain the minimum heterodyne power through the signal input and low mixer noise factor, a sufficiently high isolation between the heterodyne and signal input is required. For example, 10 dB isolation increases the noise factor of the mixer by about 10% and 10% of the heterodyne power is radiated. At 20 dB isolation, the noise factor degradation is 1% and about 1% of the local heterodyne power is radiated through the signal input of the mixer.

As can be seen in Fig. 8a, the dependence of the value of the input resistance  $R_{in}$  and the intermediate frequency  $R_{IF}$  on the power of the local heterodyne  $P_h$  in the matched load mode via the mirror channel is shown. On Fig. 8b shows the input resistance values  $R_{in}$  and IF  $R_{IF}$  depending on the power of the local heterodyne  $P_h$  in the short circuit mode ( $Y_m = \infty$ ) on the mirror channel. On Fig. 8c shows the values of the input resistance  $R_{in}$  and IF  $R_{IF}$  from the power of the local heterodyne  $P_h$  in the idle mode ( $Y_m = 0$ ) via the mirror channel. The conversion loss  $L_s$  does not depend on the external bias. In calculations, the power of the local heterodyne is related to the voltage  $U_h$  by the following expression:  $2P_h = U_h^2 / R_{in}$ .

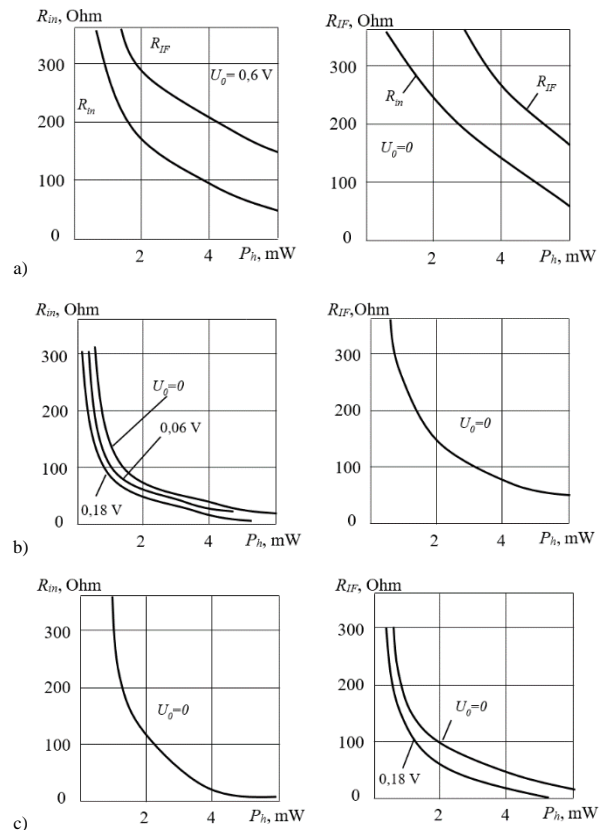


Fig. 8. The dependence of the input resistance and the IF resistance from a heterodyne power

It should be noted that the calculation and matching of the ONS should be carried out in microwave mixers, taking into account filters through the mirror channel, if any are provided in the circuits of microwave receivers. Otherwise, when the mixer is turned on in the receiving device, in which there is a filter, an inconsistency of the ONS will occur.

For example, the input conductivity of the ONS, provided that the junction capacitance  $C_j$  is a constant value, the following:

$$Y_{in} = \frac{1}{R_{in}} + j\omega C_j \approx 8.7 \times 10^{-3} + j \times 7 \times 10^{-3}$$

Then the local heterodyne power consumed by the ONS:  $P_h = U_h^2 Y_{in} / 2 \approx 2.6 \text{ mW}$ . Therefore, it is necessary to coordinate the ONS with the transmission line according to the input value  $Y_{in}$ .

When designing a microwave mixer, it is necessary to take into account the way in which the mirror frequency is usefully used. Conversion and noise factor losses can be minimized by proper choice of reactive load at signal and mirror frequencies. However, most often this is very difficult to implement, especially if the mirror and signal frequencies are close. There are two methods for solving this problem: the introduction of frequency-selective circuits and the introduction of phase relationships between signals. The circuit assembled on the basis of the first method can operate in a narrow frequency band. In addition, if the difference between the mirror frequency and the signal frequency is small, then a very high quality filter with low losses is needed. Examples of the implementation of such schemes are known, which made it possible to obtain conversion losses of up to 3.5 dB.

It should be noted that there are two signals at the mirror frequency in the mixer: the incoming signal to the input of the mixer from the antenna and the signal formed in the mixer due to the transformation of the input signal. If an external signal with a frequency  $\omega_m$  arrives at the ONS through the signal input, then, interacting with the oscillations of the local heterodyne, an intermediate frequency signal is formed  $\omega'_s = \omega_m - \omega_h$ ,  $\varphi'_s = \varphi_m - \varphi_h$ . The phase of this IF  $\varphi'_s$  is not correlated with the phase of the useful signal  $\varphi_s$ , although it does not differ in frequency from the useful signal and is an interference that cannot be eliminated without the use of special measures.

### 3. Conclusions

In conclusion, we note that in the short circuit mode through the mirror channel, the input impedance decreases significantly and reaches 50 Ohm at a power of  $3 \times 10^{-3} \text{ W}$  that is, two times less than in the matched load mode. If we take into account that the conversion loss in this case drops to 1.8 dB, then the short circuit mode in the mirror channel is the preferred mode of operation of a balanced microwave mixer. In idle mode, the mirror channel has an even lower conversion loss of 1.2 dB. It can be seen from the graphs that the resistance to the input  $R_{in}$  in the matched load mode is 50 Ohm at the local heterodyne power  $P_h = 6 \times 10^{-3} \text{ W}$ , and with external bias  $U_0 = 0.18 \text{ V}$  the input resistance is 50 Ohm at the local heterodyne power  $P_h = 4 \times 10^{-3} \text{ W}$ .

### References

- [1] Bastos L., Wietgreffe H.: Geographical Analysis of Highly Deployable Troposcatter Systems. Performance IEEE Military communications conference – MILCOM, San Diego, 2013, 661–667.
- [2] Bastos L., Wietgreffe H.: Highly-deployable troposcatter systems in support of NATO expeditionary operations. Military communications conference – MILCOM, Baltimore, 2011, 2042–2049.
- [3] Bastos L., Wietgreffe H.: Tactical troposcatter applications in challenging climate zones. Military communications conference – MILCOM, Orlando, 2012, 1–6.

- [4] Chengcheng X. et al.: Behavioral model measurement system based on signal generator and spectrum analyzer. International Conference on Microwave and Millimeter Wave Technology – ICMMT, 2021 [http://doi.org/10.1109/ICMMT52847.2021.9618281].
- [5] Chongjia H. et al.: Photonics-Based Single Sideband Mixer With Ultra-High Carrier and Sideband Suppression. IEEE Photonics Journal 13(4), 2021.
- [6] COMET – Compact Over-the-Horizon Transportable Terminal. <https://www.comtech.com/comet-compact-over-the-horizon-transportable-terminal> (available 24.09.2023).
- [7] COMET – CS67PLUS. <https://www.comtech.com/cs67plus-troposcatter-modem> (available 24.09.2023).
- [8] Hao C. et al.: All-Optical In-Phase/Quadrature Microwave Mixer for Antenna Remoting Applications. IEEE Photonics Journal 13(5), 2021, 1–7 [http://doi.org/10.1109/JPHOT.2021.3110589].
- [9] Hao C. et al.: Microwave Photonic I/Q Mixer With Phase Shifting Ability. IEEE Photonics Journal 13(4), 2021 [http://doi.org/10.1109/JPHOT.2021.3103786].
- [10] Pochernyaev V., Syvkova N.: Broadband switch on partially filled by dielectric rectangular waveguide. The scientific heritage 1(60), 2021, 49–52 [http://doi.org/10.24412/9215-0365-2021-60-1-49-52].
- [11] Pochernyaev V. M., Povkhliv V. S.: Mobile combined microwave telecommunication system. 5 International Scientific-Practical Conference Problems of Infocommunications. Scientific – Practical Conference, Kharkiv, 2018.
- [12] Pochernyaev V. N., Povkhliv V. S.: Status and directions of development of mobile digital tropospheric communication systems. Systems of arms and military equipment 2(54), 2018, 51–60.
- [13] Pochernyaev V. N., Povkhliv V. S.: Status and directions of development of mobile digital radiorelay systems. Systems of arms and military equipment 1(53), 2018, 183–188.
- [14] Pochernyaev V. M., Tsibizov K. N.: Complex waveguide theory. Scientific world, Kiev 2003.
- [15] Shilpa M. et al.: Low Noise Image-Rejection Gilbert Mixer for Software Defined Radios. IEEE International Conference on Electronics, Computing and Communication Technologies – CONECT, Bangalore 2020, 1–6 [http://doi.org/10.1109/CONECT50063.2020.9198584].
- [16] Shilpa M. et al.: Recent advancement in the design of mixers for software-defined radios. International Journal of RF and Microwave Computer-Aided Engineering 32(2), 2022, 1–20.
- [17] TALON Military Ka Band Terminal. <https://www.comtech.com/talon-gx-terminal> (available 24.09.2023).
- [18] Troposcatter and SATCOM Solutions. <https://www.comtech.com/troposcatter-and-satcom-solutions> (available 24.09.2023).
- [19] Troposcatter Antenna CSA2400. <https://www.comtech.com/troposcatter-antenna>, (available 24.09.2023).
- [20] Troposcatter Solutions <https://www.raytheonintelligenceandspace.com/what-we-do/communications-and-navigation/battlefield-comms/troposcatter> (available 24.09.2023).

**Prof. Vitaly Pochernyaev**  
e-mail: vpochernyaev@gmail.com

Doctor of Technical Sciences, professor, member of the Institute of Electrical and Electronics Engineers, professor at the National Academy of Security Service of Ukraine. Author of more than 200 publications, including 3 monographs, 2 textbooks, 12 patents for inventions.

Research interests: applied electrodynamics, radiophysics, telecommunications and radio-engineering, microwave theory and technology.

<http://orcid.org/0000-0001-7130-8668>

**Ph.D. Nataliia Syvkova**  
e-mail: natsivonat@gmail.com

Doctor of Philosophy, docent National Academy of Security Service of Ukraine. Author of more than 40 publications, including 1 textbook and 4 patents for inventions.

Research interests: telecommunications and radio-engineering, microwave theory and technology.

<http://orcid.org/0000-0002-4934-4109>

**M.Sc. Mariia Mahomedova**  
e-mail: kzk.praktika@ukr.net

Ph.D. student. Lecturer at the Kyiv Professional College of Communications. Author of more than 20 publications.

Research interests: telecommunications and radio-engineering, microwave theory and technology.

<http://orcid.org/0000-0003-1936-5555>

